Influence of skeletal classes and facial patterns on the positioning of the craniovertebral junction, dimensions of the pharyngeal airway space, and pre-vertebral soft tissue thickness: A cone beam computed tomography study

Influência das classes esqueléticas e padrões faciais no posicionamento da junção crânio-vertebral, dimensões do espaço aéreo faríngeo e espessura de tecido mole pré-vertebral: Estudo por tomografia computadorizada de feixe cônico

Influencia de las clases esqueléticas y patrones faciales sobre el posicionamiento de la unión craneovertebral, las dimensiones del espacio aéreo faríngeo y el espesor del tejido blando prevertebral: Estudio mediante tomografía computarizada de haz cónico

Received: 01/14/2024 | Revised: 01/25/2024 | Accepted: 01/26/2024 | Published: 01/30/2024

Maria Eduarda Pauly
ORCID: https://orcid.org/0009-0000-8048-3740
State University of Maringá, Brazil
E-mail: dudapauly15@gmail.com
Mariliani Chicarelli da Silva
ORCID: https://orcid.org/0000-0002-0024-7471
State University of Maringá, Brazil
E-mail: mchicarelli@gmail.com
Gustavo Nascimento de Souza Pinto
ORCID: https://orcid.org/0000-0002-6509-4998
Positivo University, Brazil
E-mail: nsouzagustavo@gmail.com
Fernanda Vessoni Iwaki
ORCID: https://orcid.org/0000-0003-0426-4313
State University of Maringá, Brazil
E-mail: fernandavessonii@gmail.com
Breno Gabriel da Silva
ORCID: https://orcid.org/0000-0002-8322-9235
University of São Paulo, Brazil
E-mail: brenogsilva@usp.br
Isabela Inoue Kussaba
ORCID: https://orcid.org/0000-0002-6833-2453
State University of Maringá, Brazil
E-mail: isabelaikussaba@gmail.com
Lilian Cristina Vessoni Iwaki
ORCID: https://orcid.org/0000-0002-1822-3056
State University of Maringá, Brazil
E-mail: lilianiwaki@gmail.con

Abstract
This study employed cone beam computed tomography (CBCT) to assess the influence of skeletal classes and facial patterns on the craniovertebral complex, pharyngeal airway space (PAS) dimensions, and pre-vertebral soft tissue thickness. The analysis of 150 CBCTs involved measurements between various vertebrae and layers of soft tissue. Significant findings included a lower odontoid process in Class II and hyperdivergent individuals, while hypodivergent subjects exhibited a larger area and volume in the PAS. A negative correlation between PAS size and pre-vertebral soft tissue thickness was observed. Gender differences were noteworthy, with males consistently displaying higher values. Significant age-related variations were also identified, with the age groups of 18-30 and 31-45 exhibiting distinct characteristics. The study underscores the impact of facial patterns and skeletal classes on the craniovertebral complex, emphasizing an inverse relationship between PAS and pre-vertebral soft tissue thickness. The intricate connections between gender and age highlight their influence on anatomical characteristics. Understanding how facial patterns and skeletal classes affect the craniovertebral complex has implications for respiratory disorders, including Obstructive Sleep Apnea and Hypopnea Syndrome (OSAHS).
Keywords: Craniovertebral junction; Prevertebral region; Cone-Beam computed tomography; Malocclusion; Pharyngeal airway space.

Resumo

Este estudo utilizou a tomografia computadorizada de feixe cônico (TCFC) para avaliar a influência das classes esqueléticas e dos padrões faciais no complexo craniovertebral, nas dimensões do espaço aéreo faríngeo (PAS) e na espessura dos tecidos moles pré-vertebrais. A análise de 150 TCFCs envolveu medições entre várias vértebras e camadas de tecidos moles. Achados significativos incluíram um processo odontoide inferior em indivíduos Classe II e hiperdivergentes, enquanto indivíduos hipodivergentes exibiram maior área e volume no PAS. Foi observada uma correlação negativa entre o tamanho do PAS e a espessura dos tecidos moles pré-vertebrais. As diferenças de género foram notáveis, com os homens apresentando consistentemente valores mais elevados. Também foram identificadas variações significativas relacionadas à idade, com as faixas etárias de 18 a 30 e 31 a 45 anos apresentando características distintas. O estudo ressalta o impacto dos padrões faciais e das classes esqueléticas no complexo craniovertebral, enfatizando uma relação inversa entre PAS e espessura dos tecidos moles pré-vertebrais. As intrincadas conexões entre gênero e idade destacam sua influência nas características anatômicas. Compreender como os padrões faciais e as classes esqueléticas afetam o complexo craniovertebral tem implicações para os distúrbios respiratórios, incluindo a Síndrome da Apneia e Hipopneia Obstrutiva do Sono (SAHOS).
Palavras-chave: Junção craniovertebral; Região pré-vertebral; Tomografia computadorizada de feixe cônico; Má oclusão; Espaço das vias aéreas faríngeas.

Resumen

Este estudio empleó tomografía computarizada de haz cónico (CBCT) para evaluar la influencia de las clases esqueléticas y los patrones faciales en el complejo craneovertebral, las dimensiones del espacio de las vías respiratorias faríngeas (PAS) y el grosor del tejido blando prevertebral. El análisis de 150 CBCT implicó mediciones entre varias vértebras y capas de tejido blando. Los hallazgos significativos incluyeron una apófisis odontoides más baja en la Clase II y en los individuos hiperdivergentes, mientras que los sujetos hipodivergentes exhibieron un área y volumen mayores en el PAS. Se observó una correlación negativa entre el tamaño del PAS y el grosor del tejido blando prevertebral. Las diferencias de género fueron notables, y los hombres mostraron consistentemente valores más altos. También se identificaron variaciones significativas relacionadas con la edad, y los grupos de edad de 18 a 30 y de 31 a 45 exhiben características distintas. El estudio subraya el impacto de los patrones faciales y las clases esqueléticas en el complejo craneovertebral, enfatizando una relación inversa entre PAS y el grosor del tejido blando prevertebral. Las intrincadas conexiones entre género y edad resaltan su influencia en las características anatómicas. Comprender cómo los patrones faciales y las clases esqueléticas afectan el complejo craneovertebral tiene implicaciones para los trastornos respiratorios, incluido el síndrome de apnea e hipopnea obstructiva del sueño (SAHOS).
Palabras clave: Unión craneovertebral; Región prevertebral; Tomografía computarizada de haz cónico; Maloclusión; Espacio de las vías respiratorias faríngeas.

1. Introduction

The odontoid process represents an anatomical structure located in the second cervical vertebra, known as the Axis. This conical projection, extending approximately 1.5 cm cranially from the body of the Axis, stands out for its anterior position to the spinal cord, playing a crucial role in anchoring the craniovertebral junction. The cranio-cervical junction is an anatomical complex that encompasses vital structures such as the brainstem, spinal cord, blood vessels, bones, and ligaments (Smoker, 1986; Cronin et al., 2009). It serves as an essential region where the skull connects to the vertebral column. The odontoid process plays a significant role in this context, providing support and stability to the head, as well as allowing a wide range of movements, including rotation, at the atlantoaxial joint. This junction, composed of the Atlas (the first cervical vertebra) and the Axis, is vital for the mobility and flexibility of the neck (Uthman et al., 2023). Previously, the diagnosis of this region was conducted through two-dimensional imaging, such as teleradiographs and lateral radiographs of the cervical region (Saunders, 1943; Hinck & Hopkins, 1960). However, the contemporary approach to evaluating this area is based on three-dimensional (3D) imaging, utilizing techniques such as computed tomography (CT) and magnetic resonance imaging (MRI) (Smoker, 1994; Agnoli & Hildebrandt, 1983; Cronin et al., 2007). These advanced modalities provide a more comprehensive and detailed view of the anatomy of the cranio-cervical junction, allowing for a more precise analysis of its structures and potential pathological conditions.

With the use of 3D technology, such as CT scans, it is possible to rapidly and accurately measure the classical lines and angles, both transverse and anteroposterior, of the foramen magnum and the vertebral canal (Cronin et al., 2007). These measurements are crucial in assessing the craniovertebral junction and defining the anatomy of the skull base, both before and after surgical interventions (Cronin et al., 2009). Three standard reference lines - Chamberlain (Chamberlain, 1939), McGregor (Mcgregor, 1948), and McRae (Mcrae, 1953) - are employed for these evaluations.

In this context, the soft tissue in the prevertebral region encompasses the distance between the anterior margin of the vertebral column and the posterior wall of the pharyngeal airway space (PAS). This linear area of soft tissue contains loose areolar tissue and lymph nodes in the retropharyngeal and retroesophageal spaces (Scarfe & Angelopoulos, 2018). Changes in this band of tissue, such as displacement or enlargement, indicate underlying cervical diseases, such as trauma or neoplasms (Chen & Bohrer, 1999; Franquet et al., 2002). Understanding the normal thickness limits of this tissue at different levels is crucial (Scarfe & Angelopoulos, 2018). Increases in soft tissue areas, such as the soft palate and tongue, can reduce the PAS, which is directly linked to Obstructive Sleep Apnea and Hypopnea Syndrome (OSAHS) and can be diagnosed by the dentist in collaboration with a multidisciplinary team (Lowe et al., 1986; Faber et al., 2019).

OSAHS is a disorder characterized by interruptions in the upper airways during sleep, which can negatively impact the patient's quality of life (Adekolu & Zinchuk, 2022; McNicholas & Pevernagie, 2022. Additionally, the PAS and the improper positioning of dental arches may be associated with the causes of this condition (Lowe et al., 1986; Faber et al., 2019). In this regard, dentists can play a crucial role in the diagnosis and treatment of OSAHS. Therefore, it is important for clinical dentists and dental radiologists to have knowledge of the normal anatomy of the prevertebral region to facilitate the diagnosis of potential pathologies in this area.

The advancement of imaging has brought significant innovations to Dentistry. Cone Beam Computed Tomography (CBCT) provides practitioners with enhanced information for diagnosis and treatment. With improvements in image quality, reduced radiation doses, and shorter image capture times, CBCT has spurred new research on maxillomandibular structures through multiplanar reconstructions. With 3D images in a 1:1 ratio, CBCT allows for a detailed evaluation of the pharyngeal airway space (PAS), distinguishing between soft and hard tissues, thus contributing to a more precise diagnosis (Di Carlo et al., 2015; Shin et al., 2015).

However, while these lines have been established for lateral radiographs, they are now being applied to CT images, but have not yet been explored in CBCT scans. Thus, this study aimed to evaluate how vertical and horizontal skeletal and facial patterns influence the positioning of the craniovertebral junction and the thickness of soft tissue in the prevertebral region in CBCT images, also considering the influence of gender and age. The hypothesis tested was that facial and skeletal patterns do not affect the positioning of the craniovertebral junction and the thickness of soft tissue in the prevertebral region.

2. Methodology

Ethics Committee

This is a retrospective study approved by the Permanent Committee on Ethics in Research Involving Human Subjects of the State University of Maringá (UEM) (CAAE: 44011321.5.0000.0104).

Image Bank

The images were consecutively selected from the examination archive of the Laboratory of Images in Clinical Research (LIPC) at UEM, covering the period from April 2014 to June 2020, totaling 150 CBCT images. These images were captured by the i-CAT Next Generation equipment (Imaging Sciences International, Hatfield, PA, USA), with a 14-bit grayscale and a focal point of 0.5 mm. For all patients, the exposure parameters used were a tube voltage of 120 kVp and a tube current ranging from 3 to 8 mA.

Inclusion criteria for this study encompassed Cone Beam Computed Tomography (CBCT) images from patients aged 18 or older, of both genders, who underwent the examination for various reasons. The included images had a Field of View (FOV) of 23x17 cm and a voxel size of 0.3 mm, covering the cranio-cervical junction to the C4 vertebra region. Patients with a history of craniofacial trauma, congenital anomalies, or prior orthognathic surgery were excluded from the study to ensure sample homogeneity. Images with missing or conflicting information in any variable, as well as those with artifacts compromising the detection or measurement of reference points, were also excluded.

Image Analysis

Two examiners with experience in CBCT conducted all assessments. A total of 150 CBCT images were analyzed using Dolphin Imaging & Management Solutions® 11.95 software, 3D version (Dolphin Imaging & Management Solutions, Chatsworth, California). This was performed on a computer equipped with the Microsoft Windows XP Professional SP-2 operating system (Microsoft Corp., Redmond, WA, USA), featuring an Intel® Core™ 2 Duo 1.86GHz-6300 processor (Intel Corporation, USA), an NVIDIA GeForce 6200 turbo cache graphics card (NVIDIA Corporation, USA), and an EIZO - S2000 FlexScan monitor with a resolution of 1600x1200 pixels (EIZO Nanao Corporation, Hakusan, Japan).

The files were transferred in DICOM (Digital Imaging and Communication in Medicine) format to Dolphin Imaging & Management Solutions® 11.95 software, 3D version, to determine horizontal and vertical skeletal discrepancies. The horizontal intermaxillary relationship was defined by the ANB angle, categorizing patients into Class I ($0° < ANB < 4°$), Class II ($ANB \geq 4°$), and Class III ($ANB \leq 0°$) (Steiner & Hills, 1953). The vertical facial pattern was established using the Jarabak quotient, which is the ratio between posterior facial height (S-Go) and anterior facial height (N-Me). This ratio categorizes patients into hyperdivergent (facial height > 0.65), normodivergent (facial height between 0.62 and 0.65), and hypodivergent (facial height < 0.62) (Sirwat & Jarabak, 1985).

To ensure standardization of the images, spatial orientation was performed by repositioning the axial plane coincidently with the Frankfurt Plane, and the median sagittal plane coincidently with the midline perpendicular to the Frankfurt Plane, passing through the cephalometric point of nasion (anterior point of the frontonasal suture) (Yamashita et al., 2017).

The following methodology was used to analyze each anatomical structure.

Position of the odontoid process

In the sagittal reconstruction, the position of the odontoid process in relation to two reference lines and anatomical points was considered (Figure 1.A):

Chamberlain's line (Saunders, 1943; Chamberlain, 1939): Extends from the posterior part of the hard palate to the posterior margin of the foramen magnum. Under normal circumstances, the odontoid process should be approximately 3 millimeters below this line (Saunders, 1943).

McRae Line: Drawn between the anterior margin of the foramen magnum (basion) to the opposite posterior edge. Under normal conditions, the odontoid process should not project above this region (Mcrae, 1953).

Measurements of the cranio-cervical junction

In the coronal (Figure 1.B) and sagittal (Figure 1.C) reconstructions, measurements were taken of the interval between the Atlas vertebra and the occipital condyle. These measurements were made from the occipital condyle to the condylar surface of the Atlas vertebra. Under normal conditions, this interval should not exceed 5 millimeters. Three measurements were taken in each reconstruction: two at the ends and one in the middle of the bone structure in question. These measurements were summed, and an average was calculated, totaling nine measurements.

Subsequently, linear measurements were made between the space formed by the Atlas vertebra and the tooth of the Axis vertebra (odontoid process). Three measurements were taken in the axial reconstruction (Figure 1.D) and another three in the sagittal reconstruction (Figure 1.E), totaling six measurements. In adults, this distance should not exceed 3 mm. Larger values indicate possible structural instability (Scarfe & Angelopoulos, 2018).

Measurement of prevertebral soft tissue thickness

In the sagittal and axial reconstructions, the measurement of prevertebral soft tissue thickness was performed at the levels of vertebrae C1, C2, C3, and C4. Three measurements were taken at each vertebra: at the highest point, the midpoint, and the lowest point of each vertebra (Figure 1.F). To confirm the measurements, at the same points in the sagittal reconstruction, measurements were taken in the axial reconstruction in the central region, corresponding to the point in the sagittal reconstruction (Figure 1.G). The values were summed, and the average per vertebra was considered.

The normative values for prevertebral soft tissue thickness, based on the book by Scarfe & Angelopoulos 2018, are: C1 ≤ 8.5 mm; C2 ≤ 6 mm; C3 and C4 ≤ 7 mm.

Volume and area of the PAS

For the evaluation of the total volume and area of the PAS, the following boundaries were established (Yamashita et al., 2017; Souza Pinto et al., 2019): a) Superior: a horizontal line drawn between the basion point and the posterior nasal spine; b) Inferior: a horizontal line passing through the lowest point of C4; c) Posterior: a vertical line passing behind the posterior wall of the PAS; d) Anterior: a vertical line passing through the soft palate, tongue, and anterior wall of the PAS.

Subsequently, the volume of the PAS was assessed at the levels of the vertebrae (C1, C2, C3, and C4), taking into consideration the upper and lower limits of each vertebra.

Group Division

For a clearer understanding of the results, the groups were divided into:

1. Classe (A):
   - b. Class I
   - c. Class II
   - d. Class III
2. Class (B):
   - a. Hyperdivergent
   - b. Hypodivergent
   - c. Normodivergent
3. Age:
   - a. 18 a 30 years
   - b. 31 a 45 years
   - c. Mais do que 45 anos
4. Sex:
   - a. Male
   - b. Female

Statistical Analysis

Intra- and inter-examiner agreements were assessed using the intraclass correlation coefficient (ICC). Normality of variables was checked with the Shapiro-Wilk test. To investigate potential differences in measurements between Classes (A) and (B), Age Groups, Lines, Vertebrae, Volume, and Area of Vertebrae, Tukey's test for mean comparison was employed when the normality assumption was met, and the non-parametric Dunn's test for median comparison when it was not. In the case of comparisons between genders, the t-Student test for mean comparison and the non-parametric Mann-Whitney test for median comparison were used, depending on the normality of the data. To investigate the effect of covariates on Chamberlain's line and McRae lines, multiple linear regression models were adjusted. The quality of these models was assessed through residual analysis and adjusted coefficient of determination. The adopted significance level was 5% (p-value < 0.05). All statistical analyses were performed using R software version 4.0.2 (R Core Team, 2020).

Figure 1 - Sagittal (A) reconstruction representing the Chamberlain's line (blue) and McRae's line (pink) in association with the odontoid process. Coronal (B) and sagittal (C) reconstructions representing the measurements taken in the interval between the Atlas vertebra and the occipital condyle. Axial (D) and sagittal (E) reconstructions, illustrating the measurements taken in the space between the Atlas vertebra and the odontoid process. Sagittal Reconstruction (F): Reference linear measurements at the highest point (a), midpoint (b), and lowest point (c) of the C3 vertebra. Axial Reconstruction (G): Linear measurement at the highest point of the C3 vertebra.

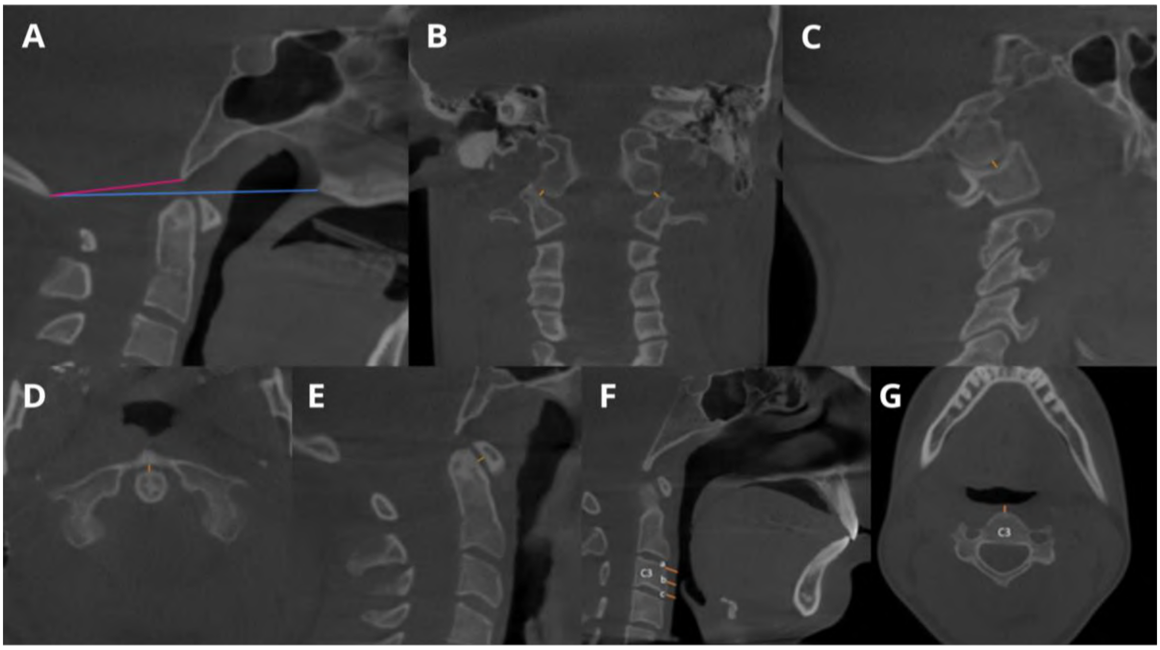

Source: Authors.

3. Results

A total of 150 CBCT scans were analyzed. Among these, 73 (48.67%) belonged to females, and 77 (51.33%) belonged to males. The mean age of the sample was 33.59 years (standard deviation ± 12.15), with a minimum age recorded of 18 years and a maximum of 64 years. For males, the mean age was 35.53 years (standard deviation ± 13.38), while for females, the mean was 31.54 years (standard deviation ± 10.41). Regarding the frequency of patients in Class (A), it is observed that Class I has 50 patients (33.00%), Class II has 47 patients (31.33%), and Class III records 53 patients (35.33%). For Class (B), the following distribution is noted: Hyperdivergent has 22 patients (14.67%), Hypodivergent has 93 patients (62.00%), and Normodivergent has 35 patients (23.33%). From the results presented in Tables 1 and 2, significant differences are observed between Classes I, II, and III only in the variables Chamberlain's line Vertebrae C3 and C4, and Areas and Volumes of Vertebrae C1 and C2 (p-value < 0.05). More pronounced values were observed for Class II in the Chamberlain's line variable, for Class I in Vertebrae C3 and C4, and for Class III in the Areas and Volumes of Vertebrae C1 and C2. When addressing comparisons between Hyperdivergent, Hypodivergent, and Normodivergent, it is noted that only the variables Chamberlain's line, Volumes of Vertebrae C1 and C3, and Total Volumes and Areas show significant differences (p-value < 0.05). Higher values were observed for Hyperdivergent in the Chamberlain's line variable, for Normodivergent in the Volume variable of Vertebra C1, and for Hypodivergent in the Volume variables of Vertebra C3 and Total Volumes and Areas.

Table 1 - Results of the comparisons of the variables under study of Class (A).

Variables	Class (A)			p-Value
	Class I	Class II	Class III	
Chamberlain's line	1,04 c	2,07 a	1,52 b	0,02*[1]
McRae's line	4,84 a	5,62 a	5,56 a	0,06[1]
Atlas – right condyle	1,04 a	1,01 a	1,08 a	0,18[2]
Atlas – left condyle	1,07 a	1,01 a	1,06 a	0,41[2]
Atlas – Axis	1,50 a	1,33 a	1,43 a	0,26[2]
C1 Soft tissue	7,06 a	6,50 a	6,76 a	0,06[2]
C2 Soft tissue	4,01 a	3,73 a	4,00 a	0,09[2]
C3 Soft tissue	3,75 a	3,46 b	3,53 b	0,006*[2]
C4 Soft tissue	4,95 a	4,03 b	3,93 bc	<0,001*[2]
EAF C1 Volume	6582,50 bc	6054,00 b	7585,00 a	0,01*[2]
EAF C2 Volume	2534,50 b	1809,00 c	3020,00 a	0,03*[2]
EAF C3 Volume	3073,00 a	2839,00 a	2730,00 a	0,77[2]
EAF C4 Volume	3778,50 a	4165,00 a	3598,00 a	0,62[2]
EAF C1 Area	273,00 ab	248,00 b	288,00 a	0,04*[2]
EAF C2 Area	123,50 b	97,00 c	129,00 a	0,01*[2]
EAF C3 Area	145,00 a	135,00 a	141,00 a	0,65[2]
EAF C4 Area	180,50 a	162,00 a	169,00 a	0,30[2]
EAF Total Volume	16402,00 a	14529,00 a	17424,00 a	0,26[2]
EAF Total Area	670,00	613,00	708,00	0,06[2]

Source: Authors.

Table 2 - Results of the comparisons of the variables under study of Class (B).

Variables	Class (B)			p-Value
	Hyperdivergent	Hypodivergent	Normodivergent	
Chamberlain's line	2,13 a	1,59 b	0,99 c	0,01*[1]
McRae's line	5,42 a	5,30 a	5,37 a	0,95[1]
Atlas – right condyle	1,03 a	1,05 a	1,05 a	0,95[2]
Atlas – left condyle	1,06 a	1,05 a	1,05 a	0,59[2]
Atlas – Axis	1,35 a	1,35 a	1,38 a	0,86[2]
C1 Soft tissue	6,48 a	7,10 a	6,76 a	0,08[2]
C2 Soft tissue	3,81 a	4,00 a	3,83 a	0,22[2]
C3 Soft tissue	3,50 a	3,66 a	3,50 a	0,10[2]
C4 Soft tissue	3,95 a	4,23 a	4,10 a	0,57[2]
EAF C1 Volume	6192,50 b	6558,00 b	7043,00 a	0,03*[2]
EAF C2 Volume	1850,00 a	2681,00 a	2322,00 a	0,34[2]
EAF C3 Volume	2621,5 b	3215,00 a	2438,00 b	0,04*[2]
EAF C4 Volume	3258,50 a	3904,00 a	3854,00 a	0,62[2]
EAF C1 Area	268,50 a	280,00 a	272,00 a	0,75[2]
EAF C2 Area	107,50 a	121,00 a	107,00 a	0,15[2]
EAF C3 Area	133,00	151,00	133,00	0,06[2]
EAF C4 Area	148,50 a	178,00 a	173,00 a	0,35[2]
EAF Total Volume	14940,50 b	16938,00 a	14363,00 b	0,02*[2]
EAF Total Area	622,00 b	718,00 a	617,00 b	0,04*[2]

*Considered significant if < 0.05; [1]Tukey's test for mean comparison; [2]Dunn's test for median comparison; Different letters indicate significance. Source: Authors. Source: Authors.

Regarding the comparisons between genders, it is noteworthy that only the variables Left Condyle Atlas, Atlas Axis, Soft Tissue at C4, and Volume of the EAF at C1 did not reveal statistical significance (p-value > 0.05). In this context, it is relevant to note that the male gender showed significant values in all conducted comparisons. Concerning the comparative analyses between age groups, it is observed that only the variables Atlas Axis, Volume of the EAF at C1, and Area of the EAF at C2 showed statistical significance (p-value < 0.05). Remarkably, significant values were identified for patients between 18 and 30 years in the variables Atlas Axis and Area C2, while patients between 31 and 45 years exhibited significant values in the variable Volume of the C1 Vertebra.

Table 3 - Result of comparisons of the variables under study of Sex.

Variables	Sex		p-Value
	Male	Female	
Chamberlain's line	2,06 a	1,04 b	0,04*[1]
McRae's line	5,83 a	4,86 b	<0,001*[1]
Atlas – right condyle	1,08 a	1,01 b	0,02*[4]
Atlas – left condyle	1,06 a	1,03 a	0,31[4]
Atlas – Axis	1,44 a	1,35 a	0,48[4]
C1 Soft tissue	7,38 a	6,26 b	<0,001*[4]
C2 Soft tissue	4,16 a	3,60 b	<0,001*[4]
C3 Soft tissue	3,73 a	3,50 b	0,03*[4]
C4 Soft tissue	4,33 a	4,08 a	0,27[4]
EAF C1 Volume	7092,00 a	6262,00 a	0,13[4]
EAF C2 Volume	2867,50 a	2198,50 b	0,01*[4]
EAF C3 Volume	3482,50 a	2448,50 b	<0,001*[4]
EAF C4 Volume	4497,50 a	3193,50 b	<0,001*[4]
EAF C1 Area	290,50 a	257,00 b	0,01*[4]
EAF C2 Area	129,50 a	101,50 b	<0,001*[4]
EAF C3 Area	178,50 a	111,00 b	<0,001*[4]
EAF C4 Area	191,00 a	141,00 b	<0,001*[4]
EAF Volume Total	18144,50 a	14138,00 b	<0,001*[4]
Total EAF Area	764,50 a	606,00 b	<0,001*[4]

Source: Authors.

Table 4 - Result of comparisons of the variables under study of Age Group.

Variables	Age range			p-Value
	18-30	31-45	>45	
Chamberlain's line	1,36 a	1,92 a	1,35 a	0,60[2]
McRae's line	5,06 a	5,56 a	5,65 a	0,17[2]
Atlas – right condyle	1,08 a	0,99 a	1,02 a	0,07[3]
Atlas – left condyle	1,06 a	1,02 a	1,00 a	0,48[3]
Atlas – Axis	1,52 a	1,25 b	1,22 b	<0,001*[3]
C1 Soft tissue	6,70 a	6,70 a	7,25 a	0,33[3]
C2 Soft tissue	3,86 a	3,93 a	3,96 a	0,79[3]
C3 Soft tissue	3,56 a	3,56 a	3,61 a	0,84[3]
C4 Soft tissue	4,33 a	4,16 a	3,90 a	0,49[3]
EAF C1 Volume	6732,50 a	7356,5 ab	5632,50 b	0,03*[3]
EAF C2 Volume	2792,50 a	2116,00 a	2165,50 a	0,06[3]
EAF C3 Volume	3042,50 a	2648,00 a	3176,50 a	0,30[3]
EAF C4 Volume	4162,50 a	3619,50 a	3342,50 a	0,36[3]
EAF C1 Area	275,00 a	278,50 a	271,00 a	0,30[3]
EAF C2 Area	127,50 a	102,00 b	103,00 b	<0,001*[3]
EAF C3 Area	134,50 a	138,50 a	178,00 a	0,10[3]
EAF C4 Area	176,50 a	172,00 a	160,50 a	0,92[3]
EAF Total Volume	17487,00 a	15591,50 a	14404,00 a	0,13[3]
EAF Total Area	666,00 a	647,00 a	725,00 a	0,83[3]

*Considered significant if < 0.05; [1] t-test for mean comparison; [2] Tukey's test for mean comparison; [3] Dunn's test for median comparison; [4] Mann-Whitney test for median comparison; Different letters indicate significance. Equations (1) and (2) represent the adjusted multiple linear regression models: (1) $\text{Chamberlain's line}_{ijkl} = \beta_0 + \beta_1 \text{ Age Group}_i + \beta_2 \text{ Class (A)}_j + \beta_3 \text{ Class (B)}_k + \beta_4 \text{ Gender}_l + \varepsilon_{ijkl}$ (2) $\text{McRae Line}_{ijkl} = \beta_0 + \beta_1 \text{ Age Group}_i + \beta_2 \text{ Class (A)}_j + \beta_3 \text{ Class (B)}_k + \beta_4 \text{ Gender}_l + \varepsilon_{ijkl}$. Source: Authors.

It is noted, in Tables 5 and 6, as well as in Figure 2, that these models exhibited satisfactory fit. This is evidenced by the Adjusted R^2, which approached 1, indicating a good explanation of variability by the models. Additionally, the residuals appeared to be randomly distributed around zero, without the identification of any trend, reinforcing the robustness and suitability of the proposed models. Regarding the obtained estimates, it is observed that for the dependent variable Chamberlain's line, Age Group (with the baseline being 18-30 years), Class (A) (with the baseline being Class I), and sex (with the baseline being Female) showed significant effects (p-value < 0.05). In other words, with an increase of one unit in the age of patients over 45 years, there is a decrease of 0.33 mm in the Chamberlain's line. In the case of patients belonging to Class II, there is an increase of 1.13 mm in the Chamberlain's line compared to patients in Class I. Furthermore, by increasing one unit in the Chamberlain's line in male patients, there is an addition of 1.26 mm in the Chamberlain's line compared to female patients (Table 3).

Table 5 - Estimates of parameters, standard error, and p-value for Model (1) considering the dependent variable Chamberlain's line.

Effects	Estimates	Standard error	p-Value	R^2 Adjusted
Intercept	-0,26	0,09	0,02*	0,94
Age range: 31-45	0,51	0,10	0,63	
Age range: >45	-0,33	0,15	0,03*	
Class II	1,13	0,14	0,04*	
Class III	0,45	0,13	0,46	
Hypodivergent	0,58	0,17	0,41	
Hyperdivergent	1,22	0,17	0,16	
Male	1,26	0,14	0,02*	

*Considered significant if < 0.05. Source: Authors.

In accordance with what was described for the dependent variable McRae's line, Age Group (with the baseline being 18-30 years), Class (A) (with the baseline being Class I), and Sex (with the baseline being Female) showed significant effects (p-value < 0.05) for the dependent variable McRae's line. With an increase of one unit in the age of patients over 45 years, an increase of 0.37 mm in the McRae's line is observed. Furthermore, it is noted that with an increase of one unit in the McRae's line in Class II patients, there is an increase of 0.88 mm in the McRae's line compared to Class I patients. Additionally, by adding one unit to the McRae's line in Class III patients, an increase of 0.69 mm in the McRae's line is observed compared to Class I patients. It is also highlighted that by adding one unit to the McRae's line in male patients, there is an increase of 0.92 mm in the McRae's line compared to female patients (Table 4).

Table 6 - Estimates of parameters, standard error, and p-value for Model (3) considering the dependent variable McRae Line.

Effects	Estimates	Standard error	p-Value	R^2 Adjusted
Intercept	4,17	0,12	<0,0001*	0,96
Age range: 31-45	0,45	0,03	0,32	
Age range: >45	0,37	0,07	0,04*	
Class II	0,88	0,14	0,01*	
Class III	0,69	0,13	0,04*	
Hypodivergent	-0,11	0,11	0,43	
Hyperdivergent	0,20	0,06	0,66	
Male	0,92	0,08	0,001*	

*Considered significant if < 0.05. Source: Authors.

Figure 2 - Residuals of the adjusted model for the dependent variables Chamberlain's line and McRae's line.

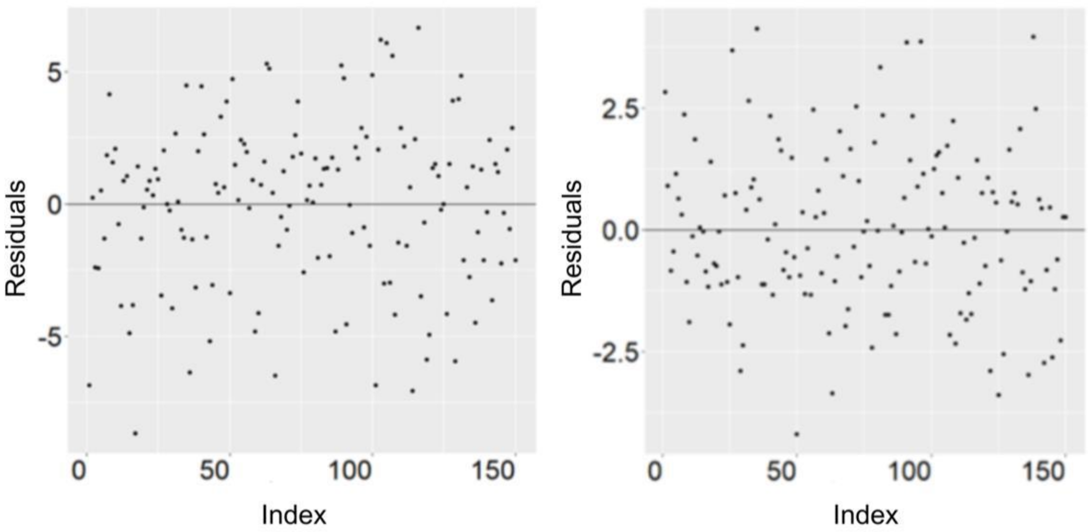

A) Pearson residuals from model (1) for Chamberlain's line.

B) Pearson residuals from model (1) for McRae's line.

Source: Authors.

It was observed that the null hypotheses that intra- and inter-examiner agreements are purely random were rejected through the intraclass correlation coefficient (ICC) for all variables under study (p-value < 0.05). In other words, intra- and inter-examiner agreements were established, with coefficients ranging from 0.84 to 0.99 (Landis & Koch, 1977).

4. Discussion

This study involved the analysis of 150 CBCT exams, with an equal distribution between male and female subjects. The mean age was 33.59 years, ranging from 18 to 64 years. Various parameters were investigated, including characteristics of Classes I, II, and III, as well as features related to vertical facial pattern. Comparisons between these classes and vertical facial patterns were statistically analyzed for craniocervical junction, PAS area and volume, and soft tissue thickness of the pre-vertebral region, along with the influence of variables such as gender and age.

The Chamberlain's and McRae's lines are anatomical reference lines drawn on imaging exams to assess the anatomy of the craniovertebral junction, measuring the protrusion of the odontoid process in relation to the foramen magnum (Cronin et al., 2009). In this study, significant differences in the position of the odontoid process were observed in Class II patients, which, on average, was situated 2.07 mm below the Chamberlain's line and 5.62 mm below the McRae's line, confirming previous findings by Cronin et al. (2009) and Tanrisever et al. (2020). Class II patients exhibited a significantly lower positioning of the odontoid process compared to Classes I and III. In comparisons between vertical facial patterns, hyperdivergent patients, especially those with a long face, showed higher values in the position of the odontoid process, particularly in relation to the Chamberlain's line, indicating a significantly lower positioning compared to other facial patterns. This analysis provided an enhanced understanding of the relationships between the anatomy of the cranio-cervical junction and the peculiarities of classes and vertical facial patterns, which may be useful in orthodontic evaluation.

The soft tissue range in the pre-vertebral region, at the level of vertebrae C3 and C4, was significantly larger in Class I patients compared to those in Classes II and III. Meanwhile, the volume of the EAF near vertebrae C1 and C2 was significantly larger in Class III patients, which also reflected in the area in that region. This relationship is inversely proportional: an increase in PAS volume and area coincides with a reduction in the thickness of the soft tissue in the pre-vertebral space. In the literature, it is observed that cases of OSAHS, a condition that can be diagnosed by the dentist and directly affects the quality and life expectancy of patients, are correlated with retrusive maxillas and mandibles, as well as an increase in soft tissue regions such as the soft palate and tongue area (Lowe et al., 1986; Faber et al., 2019). Thus, it is suggested that the soft tissue range in the pre-vertebral region should also be observed in cases of patients affected by OSAHS.

In the analyses of the total volume of the EAF, this study confirms previous findings (Di Carlos et al., 2015; Alvez et al., 2008) that did not establish statistically significant relationships between the total volume of the EAF and skeletal malocclusion. Here, only the differences in the total volume of the EAF between facial patterns were significant, showing a larger volume in hypodivergent patients, the same occurring with the total area. This understanding is crucial for radiologists, as a reduction in the volume of the EAF is associated with sleep apnea-hypopnea syndrome (OSAHS) (Franquet et al., 2002; Neelapu et al., 2017; Adekolu & Zinchuk, 2022).

In several analyzed variables, the data revealed notable discrepancies between sexes, with males showing significant values compared to females. These discrepancies point to significant anatomical differences in the morphology of the cranio-cervical junction between genders. Some variables, such as Atlas Axis, Volume of the PAS at C1, and Area of the PAS at C2, demonstrated statistical significance when compared across different age groups. These findings highlight the importance of considering not only gender but also age when assessing characteristics related to the cranio-cervical junction. Consistent with the findings of Omercikoglu et al. (2016), who evaluated cervical vertebrae according to sex and age and found significant differences, with the soft tissue range being larger in male patients and increasing with age, the authors describe that this increase may be caused by the loss of height of vertebral discs, the formation of anterior osteophytes, and regional kyphosis due to age.In a more detailed analysis, the investigation pointed out that the age group above 45 years, belonging to Class II and male gender, was associated with increases in the Chamberlain’s line. Similarly, age above 45 years, belonging to Classes II and III, and male sex were correlated with elevations in the McRae’s Line. These associations provide a more comprehensive understanding of the variables impacting the dimensions of the cranio-cervical junction and underscore the relevance of a differentiated approach considering factors such as age, skeletal classes, and vertical facial patterns.

The advent of CBCT has revolutionized the anatomical and diagnostic understanding of structures in the skull and cervical region, enabling three-dimensional visualizations in different reconstructions (coronal, sagittal, and axial). This technique allows for the observation of classical references, such as the Chamberlain’s and McRae’s lines, and provides precise details of the entire cranial structure (Smoker, 1994; Cronin et al., 2007). Additionally, CBCT provides sharper and overlap-free images, overcoming the limitations of traditional radiographs for both anatomical and pathological findings (Smoker, 1994). For the diagnosis of conditions in the craniovertebral region, CBCT is the recommended examination (Pinter et al., 2016). Proficiency in interpreting CBCT exams is crucial for dentists, particularly when assessing patients' cervical vertebral artery foramen (PAS) (Quinlan et al., 2019). These analyses play a crucial role for maxillofacial surgeons during procedures like orthognathic surgeries and for professionals seeking to accurately diagnose sleep apnea-hypopnea syndrome (OSAHS) (Elshbiny et al., 2020; Hsu et al., 2021).

The craniovertebral junction houses essential neurovascular structures. When affected by pathologies such as basilar invagination, where the odontoid process displaces into the foramen magnum, this can result in headaches and even paresthesias for the patient (Pinter et al., 2016). Often, surgical treatment becomes necessary for these cases. In this context, the evaluation of Chamberlain's line (Charmberlain, 1939) and McRae’s line (Mcrae, 1953) plays a crucial role in decision-making for surgical procedures in the region (Goel et al., 1998; Goel et al., 2004) Additionally, these lines can serve as references in the post-surgical monitoring of patients (Goel et al., 1998).

Therefore, the ability to identify potential issues in the cranio-cervical region, including the thickness of the soft tissue in the pre-vertebral region, considering patients' facial patterns, can be crucial to assist both radiologists and maxillofacial surgeons and orthodontists in diagnosing conditions such as sleep apnea-hypopnea syndrome (OSAHS). The ability to interpret imaging exams, such as CBCT, is fundamental for detecting pathologies in this area. However, there is still a suggested need for more studies that assess the cranio-cervical region and soft tissue of the pre-vertebral space using CBCT images, as there is a significant shortage in the literature on the evaluation of these structures in 3D reconstruction exams. It is essential to emphasize that, although these results provide a solid foundation, additional investigations are necessary to corroborate and expand these findings in the dental, surgical, and orthodontic scientific scenarios. The sample size is another point to be considered. Although we sought to ensure a representative sample, its limitations in terms of size may affect the generalization of results to the broader population. Future studies with more comprehensive samples are recommended to consolidate and expand the findings of this work.

5. Conclusion

This study, based on the analysis of CBCT in patients, revealed significant correlations in the morphology of the cranio-cervical junction. Class II patients showed a significantly lower odontoid process, while hyperdivergent individuals, especially those with a long face, exhibited lower positioning. The pre-vertebral soft tissue range was larger in Class I, contrasting with the larger volume of the PAS in Class III, inversely proportional to the thickness of the soft tissue. No statistical relationship was found between the total volume of the PAS and classes, but divergent facial patterns significantly influenced. Sex discrepancies were evident, with males showing marked anatomical differences. Age above 45 years, associated with male Class II, correlated with increases in the Chamberlain’s line, while male Classes II and III in this age group were associated with elevations in the McRae’s line. The study significantly contributes to the understanding of complex relationships between classes, facial patterns, and cranio-cervical anatomy. Healthcare professionals, including maxillofacial surgeons and orthodontists, can utilize these insights for a better assessment of sleep apnea-hypopnea syndrome (OSAHS). However, additional studies are recommended to validate and expand these findings, especially in CBCT exams, given the gap in the existing literature.

Acknowledgments

We express our gratitude to the State University of Maringá for the support of research and the contribution of knowledge and infrastructure for its development.

References

Adekolu, O., & Zinchuk, A. (2022) Sleep Deficiency in Obstructive Sleep Apnea. *Clin Chest Med.* 43(2), 353-371. 10.1016/j.ccm.2022.02.013.

Agnoli, L., & Hildebrandt, G. (1983) Computer-tomographic investigations in malformations of the occipito-cervical junction. *Neurosurg Rev* 6 (4), 177-85. 10.1007/BF01743099.

Alves, P. V., Zhao, L., O'Gara, M., Patel, P. K., & Bolognese, A. M. (2008) Three-dimensional cephalometric study of upper airway space in skeletal class II and III healthy patients. *J Craniofac Surg.* 19(6), 1497-507. 10.1097/SCS.0b013e31818972ef.

Chamberlain, W. E. (1939) Basilar Impression. *Yale J Biol Med.* 11(5), 487-96.

Chen, M. Y., & Bohrer, S. P. (1999) Radiographic measurement of prevertebral soft tissue thickness on lateral radiographs of the neck. *Skeletal Radiol.* 28(8), 444-6. 10.1007/s002560050543.

Cronin, C. G., Lohan, D. G., Mhuircheartigh, J. N., Meehan, C. P., Murphy, J., & Roche, C. (2009) CT evaluation of Chamberlain's, McGregor's, and McRae's skull-base lines. *Clin Radiol* 64(1), 64-9. 10.1016/j.crad.2008.03.012.

Cronin, C. G., Lohan, D. G., Mhuircheartigh, J. N., Meehan, C. P., Murphy, J. M., & Roche, C. (2007) MRI evaluation and measurement of the normal odontoid peg position. *Clin Radiol.* 62(9):897-903. 10.1016/j.crad.2007.03.008.

Di Carlo, G., Polimeni, A., Melsen, B., & Cattaneo, P. M. (2015) The relationship between upper airways and craniofacial morphology studied in 3D. A CBCT study. *Orthod Craniofac Res.* 18(1), 1-11. 10.1111/ocr.12053.

Elshebiny, T., Bous, R., Withana, T., Morcos, S., & Valiathan, M. (2020) Accuracy of Three-Dimensional Upper Airway Prediction in Orthognathic Patients Using Dolphin Three-Dimensional Software. *J Craniofac Surg.* 31(4), 1098-1100. 10.1097/SCS.0000000000006566.

Faber, J., Faber, C., & Faber, A. P. (2019) Obstructive sleep apnea in adults. *Dental Press J Orthod.* 1;24(3), 99-109. 10.1590/2177-6709.24.3.099-109.sar.

Franquet, T., Erasmus, J. J., Giménez, A., Rossi, S., & Prats, R. (2002) The retrotracheal space: normal anatomic and pathologic appearances. *Radiographics.* 22, 231-46. 10.1148/radiographics.22.suppl_1.g02oc16s231.

Goel, A. (2004) Treatment of basilar invagination by atlantoaxial joint distraction and direct lateral mass fixation. *J Neurosurg Spine.* 1(3), 281-6. 10.3171/spi.2004.1.3.0281.

Goel, A., Bhatjiwale, M., & Desai, K. (1998) Basilar invagination: a study based on 190 surgically treated patients. *J Neurosurg.* 88(6), 962-8. 10.3171/jns.1998.88.6.0962.

Hinck, V. C., & Hopkins, C. E. (1960) Measurement of the atlanto-dental interval in the adult. *Am J Roentgenol Radium Ther Nucl Med* 84, 945-51.

Hsu, W. C., Kang, K. T., Yao, C. J., Chou, C. H., Weng, W. C., Lee, P. L., & Chen, Y. J. (2021) Evaluation of Upper Airway in Children with Obstructive Sleep Apnea Using Cone-Beam Computed Tomography. *Laryngoscope.* 131(3), 680-685. 10.1002/lary.28863.

Landis, J. R., & Koch, G. G. (1977) The measurement of observer agreement for categorical data. *Biometrics.* 33(1), 159-74.

Lowe, A. A., Santamaria, J. D., Fleetham, J. A., & Price, C. (1986) Facial morphology and obstructive sleep apnea. *Am J Orthod Dentofacial Orthop.* 90(6), 484-91. 10.1016/0889-5406(86)90108-3.

McGreger, M. (1948) The significance of certain measurements of the skull in the diagnosis of basilar impression. *Br J Radiol.* 21(244):171-81. 10.1259/0007-1285-21-244-171.

McNicholas, W. T., & Pevernagie, D. (2022) Obstructive sleep apnea: transition from pathophysiology to an integrative disease model. *J Sleep Res.* 31(4), e13616. 10.1111/jsr.13616.

Mcrae, D., & Barnum, A. S. (1953) Occipitalization of the atlas. *Am J Roentgenol Radium Ther Nucl Med.* 70(1), 23-46.

Neelapu, B. C., Kharbanda, O. P., Sardana, H. K., Balachandran, R., Sardana, V., Kapoor, P., Gupta, A., & Vasamsetti, S. (2017) Craniofacial and upper airway morphology in adult obstructive sleep apnea patients: A systematic review and meta-analysis of cephalometric studies. *Sleep Med Rev.* 31, 79-90. 10.1016/j.smrv.2016.01.007.

Omercikoglu, S., Altunbas, E., Akoglu, H., Onur, O., & Denizbasi, A. (2017) Normal values of cervical vertebral measurements according to age and sex in CT. *The American journal of emergency medicine.* 35(3), 383–390. https://doi.org/10.1016/j.ajem.2016.11.019.

Pinter, N. K., McVige, J., & Mechtler, L. (2016) Basilar Invagination, Basilar Impression, and Platybasia: Clinical and Imaging Aspects. *Curr Pain Headache Rep.* 20(8), 49. 10.1007/s11916-016-0580-x.

Quinlan, C. M., Otero, H., & Tapia, I. E. (2019) Upper airway visualization in pediatric obstructive sleep apnea. *Paediatr Respir Rev.* 32, 48-54. 10.1016/j.prrv.2019.03.007.

Saunders, W. W. (1943) Basilar impression: the position of the normal odontoid. *Radiology* 41(6), 589-590.

Scarfe, W. C., & Angelopoulos, C. (2018) Maxillofacial cone beam computed tomography: principles, techniques and clinical applications, *Springer*. 10.1007/978-3-319-62061-9

Shin, J. H., Kim, M. A., Park, I. Y., & Park, Y. H. (2015) A 2-year follow-up of changes after bimaxillary surgery in patients with mandibular prognathism: 3-dimensional analysis of pharyngeal airway volume and hyoid bone position. *J Oral Maxillofac Surg.* 73(2), 340.e1-9. 10.1016/j.joms.2014.10.009.

Siriwat, P. P., & Jarabak, J. R. (1985) Malocclusion and facial morphology: is there a relationship? An epidemiologic study. *Angle Orthod.* 55(2), 127-38. 10.1043/0003-3219(1985)055<0127:MAFMIT>2.0.CO;2.

Smoker, W. R. (1994) Craniovertebral junction: normal anatomy, craniometry, and congenital anomalies. *Radiographics* 14(2), 255-77. 10.1148/radiographics.14.2.8190952.

Smoker, W. R., Keyes, W. D., Dunn, V. D., & Menezes, A. H. (1986) MRI versus conventional radiologic examinations in the evaluation of the craniovertebral and cervicomedullary junction. *Radiographics* 6(6), 953-94. 10.1148/radiographics.6.6.3317556.

Souza Pinto, G. N., Iwaki Filho, L., Previdelli, I. T. D. S., Ramos, A. L., Yamashita, A. L., Stabile, G. A. V., Stabile, C. L. P., & Iwaki, L. C. V. (2019) Three-dimensional alterations in pharyngeal airspace, soft palate, and hyoid bone of class II and class III patients submitted to bimaxillary orthognathic surgery: A retrospective study. *J Craniomaxillofac Surg*. 47(6), 883-894. 10.1016/j.jcms.2019.03.015.

Steiner, C., & Hills, B. (1953) Cephalometrics for you and me. *Am J Orthod Dentofac Orthop.* 39(10), 729-755. 10.1016/0002-9416(53)90082-7

Tanrisever, S., Orhan, M., Bahşi, İ., & Yalçin, E. D. (2020) Anatomical evaluation of the craniovertebral junction on cone-beam computed tomography images. Surg Radiol Anat. 42(7), 797-815. 10.1007/s00276-020-02457-z.

Tassanawipas, A., Mokkhavesa, S., Chatchavong, S., & Worawittayawong, P. (2005) Magnetic resonance imaging study of the craniocervical junction. *J Orthop Surg (Hong Kong)* 13(3), 228-31. 10.1177/230949900501300303.

Uthman, A., Salman, B., Shams, Aldeen, H., Marei, H., Al-Bayati, S. F., & Al-Rawi, N. H. (2023) Morphometric analysis of odontoid process among Arab population: a retrospective cone beam CT study. *PeerJ.* 11, e15411. https://doi.org/10.7717/peerj.15411

Yamashita, A. L., Iwaki Filho, L., Leite, P. C. C., Navarro, R. L., Ramos, A. L., Previdelli, I. T. S., Ribeiro, M. H. D. M., & Iwaki, L. C. V. (2017) Three-dimensional analysis of the pharyngeal airway space and hyoid bone position after orthognathic surgery. *J Craniomaxillofac Surg.* 45(9), 1408-1414. 10.1016/j.jcms.2017.06.016.